Original Article

Diabetes-Induced Activation of Canonical and Noncanonical Nuclear Factor-κB Pathways in Renal Cortex

Jonathan M. Starkey,[1] Sigmund J. Haidacher,[1] Wanda S. LeJeune,[1] Xiaoquan Zhang,[1] Brian C. Tieu,[1,2] Sanjeev Choudhary,[1] Allan R. Brasier,[1,2,3] Larry A. Denner,[1,4] and Ronald G. Tilton[1,4]

Evidence of diabetes-induced nuclear factor-κB (NF-κB) activation has been provided with DNA binding assays or nuclear localization with immunohistochemistry, but few studies have explored mechanisms involved. We examined effects of diabetes on proteins comprising NF-κB canonical and noncanonical activation pathways in the renal cortex of diabetic mice. Plasma concentrations of NF-κB–regulated cytokines were increased after 1 month of hyperglycemia, but most returned to control levels or lower by 3 months, when the same cytokines were increased significantly in renal cortex. Cytosolic content of NF-κB canonical pathway proteins did not differ between experimental groups after 3 months of diabetes, while NF-κB noncanonical pathway proteins were affected, including increased phosphorylation of inhibitor of κB kinase-α and several fold increases in NF-κB–inducing kinase and RelB, which were predominantly located in tubular epithelial cells. Nuclear content of all NF-κB pathway proteins was decreased by diabetes, with the largest change in RelB and p50 (approximately twofold decrease). Despite this decrease, measurable increases in protein binding to DNA in diabetic versus control nuclear extracts were observed with electrophoretic mobility shift assay. These results provide evidence for chronic NF-κB activation in the renal cortex of *db/db* mice and suggest a novel, diabetes-linked mechanism involving both canonical and noncanonical NF-κB pathway proteins. *Diabetes* 55:1252–1259, 2006

The concept that diabetes is a chronic inflammatory disease is supported by a growing body of clinical, epidemiological, and experimental data indicating that chronic, low-grade inflammation is a common denominator linking obesity, insulin resistance, atherosclerosis, dyslipidemia, and excessive glucose metabolism in diabetes (1–5). Epidemiological studies (2,6–8) have demonstrated that markers of inflammation predict development of both type 1 and 2 diabetes, and low-grade inflammation is now considered an important constituent of the metabolic syndrome leading to insulin resistance (9,10). The proinflammatory cytokines interleukin (IL)-6, tumor necrosis factor (TNF)-α, and IL-1β, as well as plasminogen activator inhibitor are increased in diabetic patients and are independently correlated with duration of diabetes (11,12), suggesting that chronic hyperglycemia creates a proinflammatory milieu. Even acute hyperglycemia increases circulating levels of IL-6, TNF-α, and IL-18 and exposure of human mononuclear cells obtained from healthy volunteers to elevated glucose increases TNF-α and IL-6 production (13,14).

There is a growing consensus that glucose- and diabetes-induced activation of nuclear factor-κB (NF-κB) contributes to the proinflammatory diabetic milieu (15–20). The NF-κB family of transcription factors is controlled by two distinct activation mechanisms known as canonical (classical) and noncanonical pathways (21). The former plays an important role in the host innate immune response by inducing the expression of numerous proinflammatory cytokines, chemokines, adhesion molecules, inducible enzymes, and proangiogenic growth factors as well as inhibiting apoptosis (22,23). The latter, more recently identified noncanonical pathway plays an important role in the adaptive immune response, including secondary lymphoid organogenesis and lymphocyte maturation (24,25). Noncanonical also can refer to any NF-κB gene activation pathway that does not follow the classical pathway, i.e., serine 536 phosphorylation of RelA.

The NF-κB complex is a heterogeneous collection of protein dimers in different combinations of related proteins that share a conserved DNA-binding and dimerization domain called the Rel homology domain (22). Five mammalian Rel proteins have been identified, including p65/RelA, RelB, c-Rel, p50/NF-κB1, and p52/NF-κB2. Except for p52, these proteins are constitutively present in the cytoplasm bound to a number of inhibitory proteins (inhibitor of κB [IκB]-α, IκB-β, p105, p100, and *Bcl*III) that are characterized by the presence of six to seven ankyrin repeats that mediate binding to the Rel homology domain. Both p50 and p52 exist as precursor proteins (p105 and p100, respectively), contain the ankyrin repeat structure of the inhibitory proteins, are cleaved during proteolytic processing to p50 and p52, and lack transactivation domains characteristic of the other Rel proteins (22). Stim-

From the [1]Division of Endocrinology, Department of Internal Medicine, University of Texas Medical Branch, Galveston, Texas; the [2]Department of Biochemistry and Molecular Biology, University of Texas Medical Branch, Galveston, Texas; the [3]Sealy Center for Molecular Sciences, University of Texas Medical Branch, Galveston, Texas; and the [4]Stark Diabetes Center, University of Texas Medical Branch, Galveston, Texas.

Address correspondence and reprint requests to Ronald G. Tilton, PhD, Division of Endocrinology, Department of Internal Medicine, Stark Diabetes Center, 8.138 Medical Research Building, University of Texas Medical Branch, 301 University Blvd., Galveston, TX 77555-1060. E-mail: rgtilton@utmb.edu.

Received for publication 30 November 2005 and accepted in revised form 16 February 2006.

DTT, dithiothreitol; EMSA, electrophoretic mobility shift assay; IκB, inhibitor of κB; IKK, inhibitor of κB kinase; IL, interleukin; NF-kB, nuclear factor-κB; NIK, NF-κB–inducing kinase; TNF, tumor necrosis factor.

DOI: 10.2337/db05-1554

ulation of NF-κB is mediated by diverse signal transduction cascades that converge on a large enzyme complex, the IκB kinase (IKK) (22,26). The IKK complex is composed of the catalytic subunits IKK-α, IKK-β, and the scaffold protein IKK-γ (NEMO), and like the Rel proteins, IKK-α and IKK-β undergo homo- and heterodimerization. The noncanonical NF-κB activation pathway uses IKK-α homodimers and is dependent on phosphorylation-dependent ubiquitination of NF-κB2/p100, which allows degradation of the COOH-terminal portion of the protein, freeing p52 containing the Rel homology domain (24). Activation of this pathway is initiated by an upstream mitogen-activated 3 kinase–like kinase, NF-kB–inducing kinase (NIK), and the predominant heterodimer is a p52:RelB complex (25,27).

In this study, we have quantified proteins comprising both canonical and noncanonical NF-κB activation pathways in the renal cortex of male *db/db* mice and age-matched controls. We report significant activation of the canonical pathway based on the induction of numerous NF-κB–regulated cytokines and chemokines. The increased renal cytokine production occurred without changes in canonical pathway proteins and with significant alterations in noncanonical pathway proteins. Our observations suggest that the diabetes-induced chronic activation of innate immunity may involve noncanonical NF-κB pathway proteins.

RESEARCH DESIGN AND METHODS

Male Lepr^{db} (*db/db*) mice were purchased from The Jackson Laboratories (Bar Harbor, ME) at ~4 weeks of age and were housed in the University of Texas Medical Branch Animal Resource Center in accordance with its Institutional Animal Care and Use Committee and the Public Health Service Guide for the Care and Use of Laboratory Animals. Mice with the same genetic background (C57BLKS/J) were used as controls. Mice were killed 1 and 3 months after hyperglycemia onset, defined as a group mean value >15 mmol/l, which occurred at ~8 weeks of age. Control and *db/db* mice were housed two to three per cage in a room with a 12-h artificial light cycle and free access to standard diet and water. Body weight and nonfasting blood glucose were measured weekly.

Mice were anesthetized (ketamine/xylazine; 70/10 mg/kg i.p.) and anticoagulated (5 units heparin) then exsanguinated before rapid aortic perfusion with ice-cold PBS to quickly rinse kidneys free of blood and to deliver protease (10 μg/ml pepstatin A, 10 μg/ml leupeptin, 10 μg/ml soybean trypsin inhibitor, and 10 μg/ml aprotinin) and phosphatase (1 mmol/l orthovanadate and 30 mmol/l sodium fluoride) inhibitors, phenylmethylsulphonylfluoride (1 mmol/l), and dithiothreitol (DTT) (0.5 mmol/l). Plasma was frozen at −80° C, and both kidneys were removed, decapsulated, weighed, and frozen at −80° C until processed for protein extraction. Before freezing, a 2- to 3-mm midline transmural section was removed from each kidney for fixation in 10% formaldehyde for 24 h before processing for immunohistochemistry.

Metabolic and cytokine measurements. Commercially available kits were used to measure plasma glucose (Sigma-Aldrich, St. Louis, MO), cholesterol, and triglycerides (Wako Chemicals, Richmond, VA). Insulin, leptin, and amylin (Linco, St. Louis, MO) and multiple cytokines and chemokines were measured on additional aliquots of plasma and on a sample of renal cortical extract collected after 3 months of hyperglycemia using the Bio-Plex system, which are multiplex bead-based assays used with the Luminex xMAP technology according to the manufacturer's instructions (Bio-Rad Laboratories, Hercules, CA). Eight-point standard curves were performed for each cytokine using the same Luminex bead technology.

Preparation of cytosolic and nuclear protein extracts. Renal cortex (~50 mg) was homogenized on ice using Wheaton 1-ml Dounce homogenizers in a 20-fold excess (wt/vol) of low-salt solution A (50 mmol/l HEPES, pH 7.0, 10 mmol/l KCl, 1 mmol/l EDTA, 1 mmol/l EGTA, protease inhibitor cocktail [Sigma P8340, containing 240 μg/ml AEBSF, 5 μg/ml aprotinin, 10 μg/ml leupeptin, 14 μg/ml bestatin, 10 μg/ml pepstatin A, and 5 μg/ml E-64], phosphatase inhibitors [1 mmol/l orthovanadate and 30 mmol/l sodium fluoride], 1 mmol/l DTT, and 0.5 mmol/l phenylmethylsulphonylfluoride). The homogenate was spun for 30 s at 100*g* and 4°C to remove tissue debris, the supernatant was transferred to a fresh tube, 10% NP-40 was added for a final concentration of 0.05%, tubes were mixed by gentle inversion, and immediately spun for 7 min at 1,000*g* and 4°C. The supernatant was used as cytosolic extract, while the pellet was gently resuspended in solution A containing 1 mol/l sucrose, and spun for 5 min at 8,000*g* at 4°C. The supernatant was removed and discarded, and the pellet gently resuspended in 20 μl solution A. Eighty microliters of a high-salt solution B (50 mmol/l HEPES, pH 7.0, 500 mmol/l KCl, 1 mmol/l EDTA, 1 mmol/l EGTA, 10% glycerol, protease and phosphatase inhibitors, 1 mmol/l DTT, and 0.5 mmol/l phenylmethylsulphonylfluoride) were added dropwise with gentle vortexing. The suspension was allowed to sit on ice for 30 min, vortexing for 15 s every 5 min, then spun at 16,100*g* for 20 min. The supernatant was used as nuclear extract. Protein concentrations of nuclear and cytosolic extracts were determined using the Bio-Rad (Hercules, CA) protein assay with bovine albumin standards, and both samples were assayed for cytosolic (β-tubulin and glyceraldehyde-3-phosphate dehydrogenase) and nuclear (lamin B) proteins.

TABLE 1
Primary antibodies for NF-κB protein detection by Western blot

Protein	Species	Antibody dilution	Mouse kDa band
Canonical NF-κB proteins			
RelA/p65			
Santa Cruz sc372	Goat	1:500	60
Novus Biological ab7970	Rabbit	1:1,000	
Rockland 100-4165	Rabbit	1:4,000	
p50			
Cell Signaling 3035	Rabbit	1:500	50
Calbiochem PC136	Rabbit	1:500	
Santa Cruz sc114	Rabbit	1:1,000	
IκB-α			35
Santa Cruz sc371	Rabbit	1:500	
Rockland 100-4167C	Rabbit	1:4,000	
IκB-β			
Santa Cruz sc945	Rabbit	1:1,000	38
Rockland 100-4186	Rabbit	1:4,000	
IKK-β			
Santa Cruz sc8014	Mouse	1:1,000	84–85
Calbiochem OP134	Mouse	1:500	
Noncanonical NF-κB proteins			
RelB			
Cell Signaling 4954	Rabbit	1:1,000	60
Santa Cruz sc 226*	Rabbit	1:500	
p52			
Upstate 05361	Rabbit	1:500	44–45
Santa Cruz sc298	Rabbit	1:500	
NIK			
Biovision		1:1,000	103
Cell Signaling 4994	Rabbit	1:1,000	
IKK-α			
Calbiochem OP133	Mouse	1:500	84–85
Santa Cruz sc7607		1:1,000	

*RelB antibody (sc226) was obtained from lot number L0204. Subsequent lots of this antibody are less immunoreactive for RelB in mouse renal cortical extracts.

Western immunoblot analysis. Western blots were quantified from three to five separate sets of cytosolic and nuclear protein extracts pooled from an equal mass of renal cortical extract of three control and three diabetic animals using a panel of antibodies for each mouse protein (Table 1). Tissue lysates were electrophoresed on 7.5 or 10% SDS-polyacrylamide gels and analyzed by immunoblotting after transfer to nitrocellulose membranes (Bio-Rad), using primary antibodies according to each manufacturer's instructions, followed by species-specific secondary antibodies tagged with a fluorescent dye (IR Dye 800; Rockland) at a 1:5,000 dilution. Densitometric quantitation of each protein was performed using the LI-COR Bioscience Odyssey Imaging System with infared fluorescence detection (LI-COR Bioscience, Lincoln, NE). β-Actin was measured on every blot using an IR Dye 700 for evaluation of protein loading.

Electrophoretic mobility shift assay. Sense and antisense oligonucleotides containing an IL-6 NF-κB consensus sequence (5′-CATGTGGGATTTTCCCATGAC-3′) with a 5′ IR Dye 700 label were purchased, and double-stranded DNA was prepared according to the manufacturer's instructions (LI-COR Bio-

science). An IR Dye 800–labeled mutant oligonucleotide (5′-CATGT GAGATTTTCACATGAC-3′) was used as a control. Unlabeled (cWT) IL-6 promoter was purchased from Sigma Genosys. A total of 17.5 μg nuclear extract were diluted to a concentration of 4 μg/μl by the addition of solution C (1:4 solutions A:B) then combined with 2 μl ice-cold 10× binding buffer (100 mmol/l TRIS, 500 mmol/l NaCl, 10 mmol/l DTT, pH 7.5) and Milli-Q water to make a final volume of 20 μl. Where applicable, 80-fold excess unlabeled wild-type oligonucleotide or 80-fold excess mutant oligonucleotide were added to the mixture and allowed to equilibrate for 15 min. One microliter of fluorescent probe was added and allowed to equilibrate on ice for 30 min. Samples were mixed with 1 μl loading dye, placed on a 4% native PAGE gel, and the gel was run at 160 V on ice for 1 h then imaged using the LI-COR Bioscience Odyssey Imaging System according to the manufacturer's instructions. RelB (Santa Cruz 226×; 4 μg), p50 (Santa Cruz 114×; 4 μg), and p65 (600-401-271, 2 μg; Rockland) antibodies were separately added to the incubation mix for 30 min at room temperature before adding probe to perform supershift assays.

Immunohistochemistry. Paraffin-embedded 5-μm kidney sections were washed in xylene twice for 5 min each and rehydrated by successive rinsing in 100, 95, 75, and 50% ethanol followed by PBS, and antigen retrieval was performed using 10 mmol/l sodium citrate (pH 6.0) with 0.1% Triton X for 20 min at 95°C. Slides were blocked using nonimmune sera from the secondary antibody species diluted to 2% in PBS containing 0.2% cold fish skin gelatin, 0.1% saponin, and 0.05% Tween 20 for 2 h at room temperature. Primary antibodies directed against NIK (Cell Signaling 4994, 1:100 dilution), RelB (sc226, 1;100 dilution; Santa Cruz Biotechnology), p50 (Abcam 7971, 1:100 dilution), F4/80 (specific macrophage stain, 1:100 dilution; Abcam 16911), and myeloperoxidase (specific neutrophil stain,1:500 dilution; Spring Bioscience) were incubated overnight at 4°C in blocking buffer containing 2% BSA substituted for the nonimmune sera. Tissue sections were washed three times in PBS for 10 min each, and secondary antibody Texas Red–labeled goat anti-rabbit IgG (1:100 dilution; Rockland) was added for 2 h at room temperature. Sections were again washed three times in PBS, and DAPI (1:10,000 dilution of a 100-μg/ml stock in PBS) was added for 15 min for nuclear counterstaining, the sections washed in PBS, mounted with coverslips, and viewed using a Nikon Eclipse 80*i* microscope with fluorescence illumination system and digital camera (DXM1200F). Negative controls included omitting the primary antibody.

RESULTS

Gravimetric, metabolic, and hormone data. Body weights of *db/db* mice were increased significantly at the onset of hyperglycemia, peaked by 1 month of hyperglycemia (approximately twofold increase over age-matched controls), then remained constant over the next 2 months (Table 2). After 3 months of hyperglycemia, the *db/db* mice exhibited significant hypercholesterolemia, hyperinsulinemia, and hyperleptinemia, and plasma amylin levels were increased ~10-fold versus control mice (Table 2).

Plasma and renal tissue cytokine levels. Numerous cytokines and chemokines were significantly increased in plasma of diabetic versus control mice after 1 month of hyperglycemia, including RANTES (40% increase), IL-1α (45%), IL-1β (50%), IL-12(p70) (60%), TNF-α (62%), IL-3 (84%), and IL12(p40) (100%) (Fig. 1). After 3 months of hyperglycemia, all of these cytokines were decreased 50–80% below controls, while additional cytokines were increased approximately twofold, including KC, IL-6, G-CSF ($P < 0.05$ vs. controls), and MIP-1α. Numerous proinflammatory cytokines were increased significantly in 3-month renal cortical extracts, ranging from a 14% increase for IL-2 to a threefold increase for KC (Fig. 2). In addition, anti-inflammatory cytokines, including IL-12(p40) and IL-10, were significantly decreased.

Western blot of NF-κB pathway proteins. Band intensities of NF-κB pathway proteins were quantified from separate renal cortical cytosolic and nuclear extracts from mice diabetic for 3 months and their age-matched controls (Fig. 3). Results are expressed as a mean and SD of the ratio of diabetic to control band intensities after normalization to β-actin from each lane. Quantitation of three separate sets of pooled extracts from three control and three diabetic mice revealed no significant change in band intensities for RelA/p65 (1.00 ± 0.19), p50 (1.03 ± 0.20), IκB-α (1.07 ± 0.12), and IκB-β (1.14 ± 0.09) in the canonical pathway, while NIK and RelB were increased 5.6-fold and 3-fold, and IKK-α was decreased 38%. The nuclear content of canonical and noncanonical NF-κB pathway proteins was decreased in diabetic renal cortex (Fig. 3). RelB increased threefold in the cytoplasm and decreased twofold in the nucleus of diabetic versus control mice (Fig. 4*A*). Under the experimental conditions utilized for Western immunoblotting, p100 was identifiable only in nuclear extracts (Fig. 4*B*) and in general was not visible on Western blots from total tissue extracts in which the nuclear proteins would be diluted into the much larger volume of cytosolic proteins (data not shown). p52 could not be reproducibly measured.

TABLE 2
Gravimetric, metabolic, and hormone data for *db/db* mice

Measurement	Control	*db/db*
n	12	12
Body weight (g)		
Initial	18.8 ± 1.3	25.9 ± 5.5*
1 month	23.4 ± 1.6	45.7 ± 3.6†
3 months	26.0 ± 1.8	46.1 ± 8.5†
Blood glucose (mmol/l)		
Initial	8.7 ± 1.2	14.0 ± 8.7
1 month	7.2 ± 1.4	25.1 ± 5.3†
3 months	7.0 ± 0.9	31.7 ± 3.7†
Cholesterol (mmol/l)		
3 months	1.92 ± 0.21	2.56 ± 0.66‡
Hormone levels (pmol/l)		
Insulin	127 ± 93	374 ± 353‡
Leptin	63 ± 15	382 ± 194†
Amylin	6 ± 3	56 ± 29†

Data are means ± SD. Hormone levels measured after 3 months of hyperglycemia with the LINCOplex kit according to manufacturer's instructions. Significantly different from controls by Students *t* test: *$P < 0.001$; †$P < 0.0001$; ‡$P < 0.01$.

Analysis of phosphorylation sites on NF-κB pathway proteins from whole-tissue extracts indicated that phosphorylation of serines 276, 529, and 536 on RelA/p65 was decreased in diabetic versus control tissue (Fig. 4*C*). Likewise, separate antibodies recognizing serine 32 or serines 32 and 36 of IκB-α indicated either no change or decreases in diabetic renal cortex. In contrast, antibodies recognizing phosphorylation sites of IKK-α (serines 176 and 180) and IKK-β (serines 177 and 181) indicated increased phosphorylation in diabetic renal cortex.

Electrophoretic mobility shift assay. Increased binding of protein to DNA was observed in nuclear extracts of diabetic versus control renal cortex (Fig. 5, *lanes 2* vs. *5*). A single complex was identified that was specifically inhibited by an 80-fold excess of cold wild-type oligonucleotide (*lanes 3* and *6*) but not by the same excess of mutant oligonucleotide (*lanes 4* and *7*). Antibodies to RelB were capable of supershifting a portion of the protein binding to the DNA (*lane 8*), while antibodies to RelA and p50 did not, even though the latter antibodies were capable of gel shifting TNF-α–stimulated Hela cell complexes (data not shown).

Immunohistochemistry. Immunostaining for NIK demonstrated renal tubular epithelial localization in kidney sections from both control and diabetic mice (Fig. 6*B* and

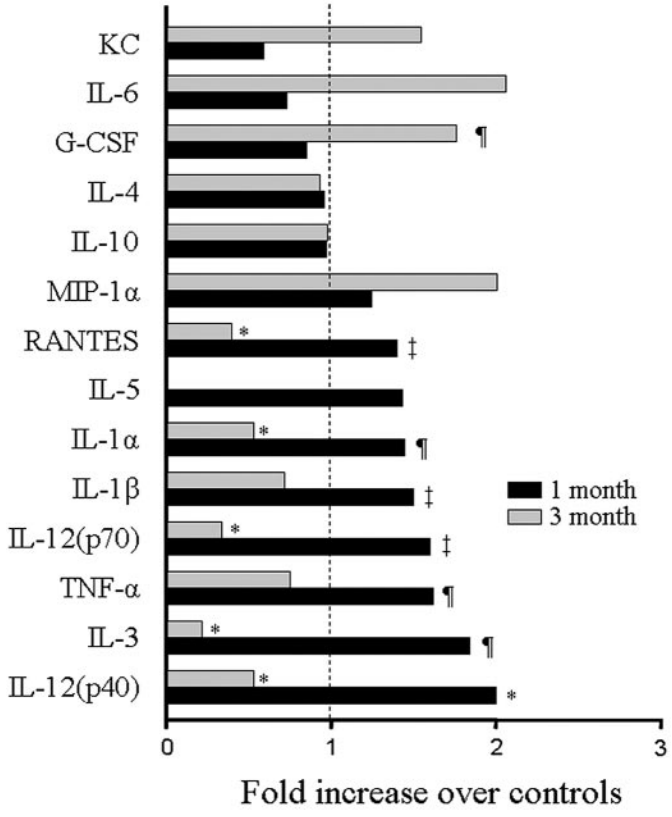

FIG. 1. Diabetes affects plasma levels of cytokines and chemokines. Plasma samples collected after 1 and 3 months of diabetes and expressed as fold change over nondiabetic controls. Cytokines arranged in order of increasing fold change for 1-month samples. Control, 1 and 3 months: $n = 18$; diabetic 1 month: $n = 10$; and diabetic 3 months: $n = 17$. Significantly different from controls by Student's t test: *$P < 0.0001$; †$P < 0.001$; ‡$P < 0.01$; ¶$P < 0.05$.

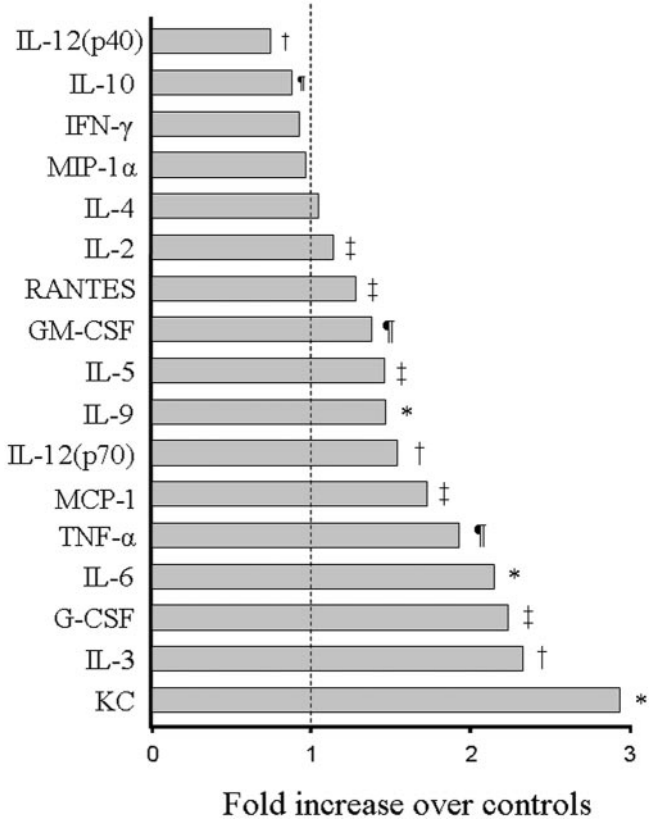

FIG. 2. Diabetes increases NF-κB–regulated cytokines in renal cortex. Renal cortical extracts after 3 months of diabetes with cytokines expressed as fold change over nondiabetic controls. Cytokines arranged in order of increasing fold change. $n = 15$ for control and diabetic groups. Significantly different from controls by Student's t test: *$P < 0.0001$; †$P < 0.001$; ‡$P < 0.01$; ¶$P < 0.05$.

C). In control mice, NIK staining was predominantly located near the basal aspect of proximal tubular epithelial cells (Fig. 6*B*). Distal tubules, glomeruli, and interstitial cells remained relatively unstained (Fig. 6*B*, arrowheads), as did nuclei. The cellular distribution of NIK was comparable in diabetic kidneys, although there was increased staining throughout proximal tubular epithelial cells (Fig. 6*C*). RelB staining was intense and predominantly located in proximal and distal tubular epithelial cells in both control and diabetic mice (Fig. 6*E* and *F*). Nuclear staining was present within controls (arrowheads) but much less evident within diabetic kidneys. RelB staining was present but much lighter within glomeruli (Fig. 6*F*). p50 was present within renal tubular epithelial cells but not glomeruli of both control and diabetic kidneys, although the distribution of staining was punctuate and not very common (Fig. 6*H* and *I*).

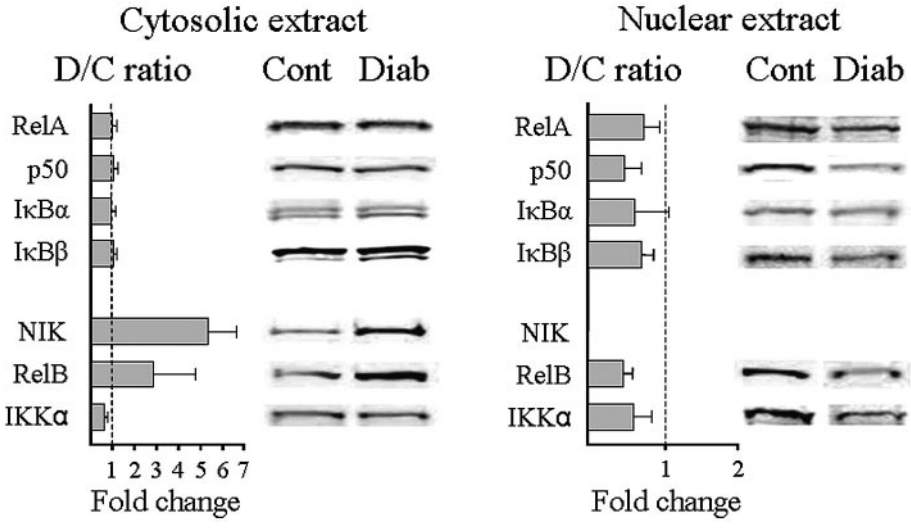

FIG. 3. Cytosolic and nuclear extracts were prepared from 3-month diabetic and age-matched control mouse kidneys. An equal amount of protein was pooled from three control and three diabetic mice, and three separate sets were used for densitometric quantitation of each protein. Results are expressed as a mean and SD of the ratio of diabetic to control band intensities (D/C ratio) after normalization to β-actin from each lane. Representative Western blots are shown for each protein. Under the experimental conditions used (50 μg/lane), NIK was not measurable in nuclear extracts.

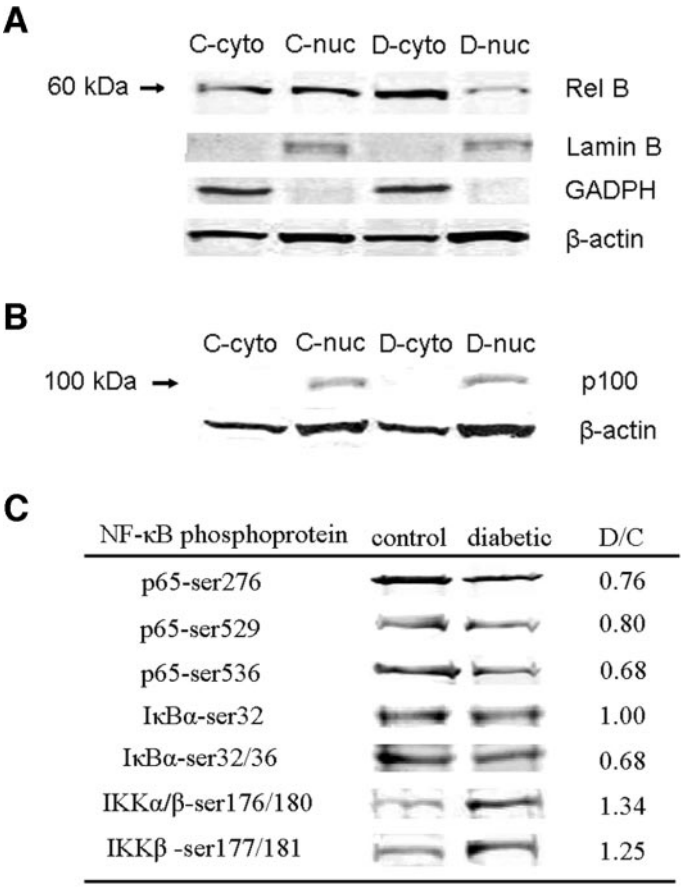

FIG. 4. *A*: Representative Western immunoblots demonstrating RelB increases in the cytoplasm of diabetic mice and a corresponding loss of nuclear RelB in diabetic mice. Representative blots for lamin B (nuclear protein) and glyceraldehyde-3-phosphate dehydrogenase (GAPDH) (cytoplasmic protein) are shown demonstrating the purity of cytosolic versus nuclear protein separation. β-Actin is loading control. *B*: Western immunoblot of p100 demonstrating its nuclear localization. β-Actin is loading control. *C*: Analysis of activating phosphorylation sites on selected NF-κB pathway proteins (RelA/p65, IκB-α, IKK-α, and IKK-β) from protein extracts obtained from the renal cortex of 3-month diabetic and age-matched control mice. Representative Western immunoblots are shown, and the D/C ratio represents values from three separate mice for each experimental group.

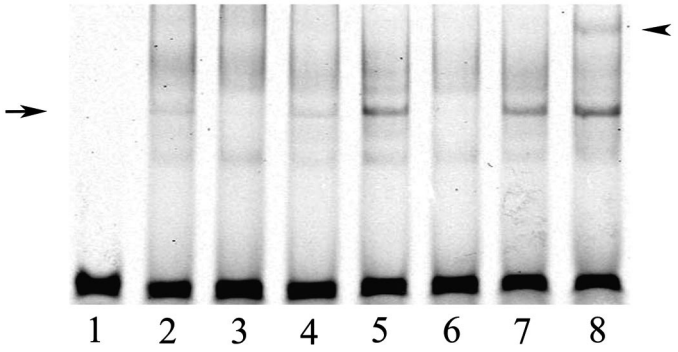

FIG. 5. EMSA demonstrating increased protein binding (arrow) in diabetic versus control nuclear extracts sampled from 3-month diabetic versus age-matched control mice. *Lane 1*: unlabeled oligo. *Lane 2*: control nuclear extract. *Lane 3*: control plus 80-fold molar excess of cold oligo. *Lane 4*: control plus 80-fold molar excess of mutant oligo. *Lane 5*: diabetic nuclear extract. *Lane 6*: diabetic plus 80-fold molar excess of cold oligo. *Lane 7*: diabetic plus 80-fold molar excess of mutant oligo. *Lane 8*: RelB supershift (arrowhead) using Santa Cruz anti-RelB antibody (sc226).

DISCUSSION

Diabetes-induced inflammation and renal cytokine production. This study utilized the *db/db* mouse model of type 2 diabetes since it develops robust changes within 2 months of the onset of hyperglycemia that include increases in renal mass, glomerular volume, mesangial volume, glomerular filtration rate, basement membrane thickening, and urinary albumin excretion (28). Our observation that numerous cytokines and chemokines, previously shown to be regulated in part by canonical NF-κB pathway activation (23,29), were increased in the renal cortex of diabetic mice indicates chronic activation of the innate immune response via this NF-κB pathway. Several of the elevated cytokines and chemokines previously have been associated with diabetic nephropathy (TNF-α, IL-6, MCP-1, and RANTES) (30), while many have not (IL-2, IL-3, IL-5, IL-9, IL-12, G-CSF, GM-CSF, and KC). Virtually all cytokines and chemokines listed in Figs. 1 and 2 contain κB motifs within the promoter region of their DNA (23). Exceptions include IL-3, IL-4, and IL-5, which are regulated by nuclear factor of activated T-cells (29). These elevated cytokines represent renal production of cytokines and not plasma contamination since kidneys were rinsed free of blood and plasma levels of the tested cytokines were at or below control levels at the 3-month time point. The possibility that infiltrating neutrophils, monocytes, and macrophages are responsible for the cytokine production cannot be ruled out but appears unlikely given the low numbers of infiltrating macrophages previously reported at this time point (31), and our inability to demonstrate a significant diabetes-induced increase of either macrophages (using anti-F4/80 antibody) or neutrophils (using anti-myeloperoxidase antibody) in random kidney sections from *db/db* mice (data not shown). The major contribution of tubular epithelial cells to total NF-κB protein content demonstrated with immunohistochemistry in this study, together with previous observations that tubular epithelial cells produce a variety of cytokines and chemokines in other renal inflammatory diseases (32), suggest that this cell is responsible for the diabetes-induced increased cytokine production. We are the first to report that NIK and RelB are predominantly localized to tubular epithelial cells, an observation strikingly similar to other renal inflammatory diseases (see below).

Diabetes-induced canonical NF-κB activation. Increased immunohistochemical localization of p50 and p65 in the nucleus has been used as evidence of diabetes-induced activation of NF-κB (18–20). Likewise, reports using electrophoretic mobility shift assays (EMSAs) on cell extracts from renal and vascular cells in tissue culture have provided evidence of glucose-induced activation of NF-κB (15–19). A major caveat of these approaches is that NF-κB protein binding is not synonymous with transcriptional activation, and demonstrating nuclear localization and/or DNA binding via these two methods provides no insights into mechanisms of diabetes-induced NF-κB transcriptional activation.

Within the kidney, most studies of NF-κB activation have utilized mesangial cells exposed to a variety of stimuli in tissue culture (rev. in 17) and have evaluated RelA and p50 as the predominant NF-κB proteins. Renal tubular epithelial cells have received less attention, although recent studies (19,33) have demonstrated active NF-κB. Even fewer experimental animal studies (20,34,35)

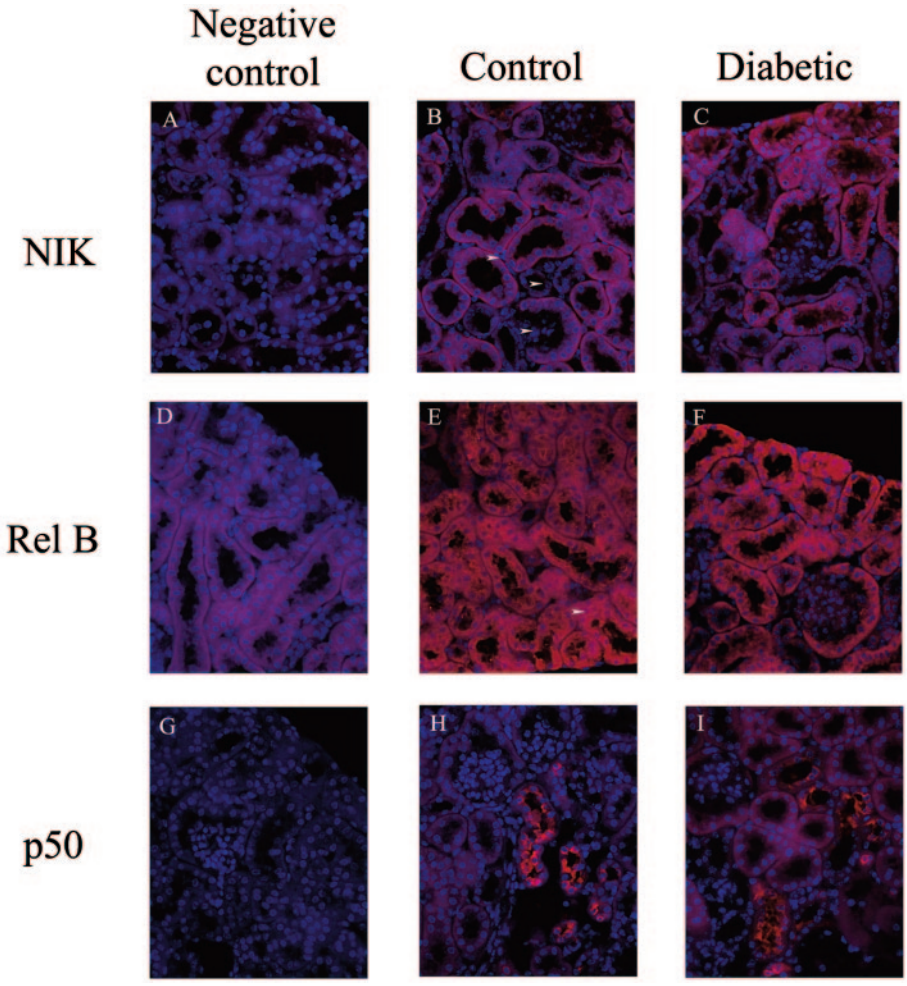

FIG. 6. Representative 5-μm formalin-fixed sections of kidney sampled from control (*B*, *E*, and *H*) and diabetic (*C*, *F*, and *I*) mice. Negative controls (eliminating the primary antibody) are shown for the diabetic tissues in *A*, *D*, and *G*. Secondary antibody used for both NIK and RelB was Texas Red–conjugated antibody. While NIK was predominantly located in proximal tubular epithelial cells in controls and diabetics, RelB staining was distributed throughout all tubules in the cortex. Little immunostaining was observed in the glomeruli for NIK and RelB. p50 immunostaining was localized to only a few tubules in each section of control and diabetic kidneys. ×400 magnification.

have evaluated renal NF-κB activation, and results are more discordant than in vitro cell culture studies. Reasons for this may include more chronic exposure to hyperglycemia, diabetes models evaluated (type 1 vs. type 2), animal species, and more complex tissue extracts than single-cell culture systems. Despite the decreased amounts of all NF-κB proteins in nuclear extracts of 3-month diabetic *db/db* mice, we also report an increased protein binding to DNA using EMSA. While paradoxical, these data are consistent with the observation that the pool of individual nuclear NF-κB proteins is much larger than the total amount of NF-κB proteins actually binding to DNA (36). In contrast to previous experiments, only RelB could be supershifted slightly. Several possibilities exist for the inability of RelA and p50 antibodies to supershift the DNA-binding complex. These possibilities include the following: *1*) RelA is incapable of binding DNA, perhaps through formation of inactive heterodimers with RelB (37), and *2*) antibody epitopes are inaccessible in the protein complex.

The absence of any significant detectable changes by Western blot in cytosolic NF-κB pathway proteins comprising the canonical pathway, and the finding that nuclear levels of all NF-κB pathway proteins were decreased by approximately one-half, indicate that diabetes-induced chronic activation of the innate immune response is neither dependent on significant movement of NF-κB dimers into the nucleus, nor is it due to prolonged degradation of IκB inhibitory proteins that function to keep RelA:p50 homo- and/or heterodimers in the cytoplasm. The latter observation is consistent with previous reports showing sustained NF-κB activation in the absence of significant decreases in IκB-α expression in peripheral blood mononuclear cells exposed to chronic high glucose (18).

Noncanonical NF-kB activation pathway. The major novel finding of this study is diabetes-induced dysregulation of the noncanonical NF-κB activation pathway, including significant changes in NIK, RelB, and IKK-α. Our finding in diabetic kidneys that cytosolic and nuclear IKK-α was decreased ~40% (Fig. 3) yet phosphorylated IKK-α was increased 34% (Fig. 4*C*) indicates that the fraction of activated IKK-α increased significantly and provides support for noncanonical NF-κB pathway activation. While only a few noncanonical pathway target genes have been identified, the positive transcriptional role of this pathway is clearly manifested in mice lacking specific noncanonical NF-κB proteins (38). Pathophysiological roles for NIK remain mostly unexplored and the significance of the several-fold increase in NIK in diabetic renal cortex remains unclear at this time. NIK activation has been reported in pig models of ischemia-reperfusion injury and in delayed graft function in patients receiving kidney transplants (39). In the latter, activation of NIK occurred within proximal tubular epithelial cells, in a pattern strikingly similar to diabetes-induced changes reported here. In addition, NIK activity was induced by thrombin in cultured proximal tubular epithelial cells (39).

RelB displays a number of unusual features compared with other Rel proteins; it is weakly controlled by IκB proteins and can serve as both a promoter and repressor of NF-κB–dependent gene expression (22,23,40). RelB primarily forms complexes with p50 and p52, the only Rel proteins lacking transactivation domains, yet is a transcriptional activator in these dimer conformations. Previously, it has been shown to be constitutively present only in nuclei of immune cells (40), and we show here that this also is true for renal cells (Fig. 3). Like IκB proteins, the expression of RelB is controlled by NF-κB (41), and the threefold increase in cytosolic RelB reported in this study is consistent with NF-κB canonical pathway activation.

Potential mechanisms responsible for prolonged activation of the NF-κB canonical pathway in diabetic kidney. At least three potential mechanisms may contribute to the prolonged activation of the canonical NF-κB pathway observed in renal cortex of *db/db* mice. First, based on the phenotype of RelB-deficient mice, RelB has been implicated as an important repressor of the inflammatory process, modulating the transition from innate to adaptive immunity (42). These mice develop a severe, noninfectious, multiorgan inflammatory syndrome that significantly contributes to their premature death (43). Renal fibroblasts harvested from RelB-deficient mice exhibit dysregulated cytokine production following LPS stimulation, which can be corrected by transfection of RelB cDNA into these cells (42). At least two mechanisms may be responsible for the repressive function of RelB. First, it has been reported that RelB exerts transcriptional suppression via stabilization of IκB-α protein (44). A second mechanism is via inhibition of DNA binding by RelA through its complex formation with RelB (37). Despite the threefold increase in cytosolic RelB, the nuclear content was decreased twofold in diabetic kidneys, which may be sufficient to impact upon its ability to form dimers with IκB-α or RelA to terminate the innate immune response. A second potential mechanism for the diabetes-induced prolonged activation of the canonical NF-κB pathway involves phosphorylation of RelA ser276, which is necessary for RelA/RelB dimerization (45). We report a decrease in ser276 phosphorylation in diabetic kidney (Fig. 4*C*). Third, it has recently been reported that IKK-α plays a negative role in macrophage activation and inflammation by accelerating the turnover and removal of RelA from proinflammatory gene promoters (46). This was accomplished via phosphorylation of RelA ser536; impaired ser536 phosphorylation significantly prolonged the retention time of RelA on the promoter of NF-κB genes. It is noteworthy that both IKK-α protein levels (cytosolic and nuclear) and RelA ser536 phosphorylation were decreased in diabetic kidneys in this study.

In summary, we report sustained activation of innate immunity via the NF-κB canonical pathway in the renal cortex of *db/db* mice after 3 months of hyperglycemia, manifested by significantly elevated tissue concentrations of numerous NF-κB–regulated cytokines and chemokines. This was associated with a twofold reduction in the nuclear content of all NF-kB pathway proteins, no changes in tissue cytosolic levels of all proteins comprising the canonical pathway, and with significant changes in proteins essential for noncanonical NF-κB pathway activation, including NIK, IKK-α, and RelB.

ACKNOWLEDGMENTS

This project was supported by an American Diabetes Association Research Grant (to R.G.T.) and a National Heart, Lung, and Blood Institute Grant HL055630 (to A.R.B.). B.C.T. is a recipient of a National Institute of Environmental Health Sciences Predoctoral Training Grant (M. Moslen, Director) and a McLaughlin Predoctoral Fellowship in Infection and Immunity (Stanley M. Lemon, Director).

We acknowledge the excellent technical assistance of Hung Sun, Hung Q. Doan, Negin N. Fouladi, and Chang Lee.

REFERENCES

1. Pickup JC, Crook MA: Is type II diabetes mellitus a disease of the innate immune system? *Diabetologia* 41:1241–1248, 1998
2. Schmidt MI, Duncan BB, Sharrett AR, Lindberg G, Savage PJ, Offenbacher S, Azambuja MI, Heiss G: Markers of inflammation and prediction of diabetes mellitus in adults (Atherosclerosis Risk in Communities Study): a cohort study. *Lancet* 353:1649–1652, 1999
3. Fernández-Real JM, Ricart W: Insulin resistance and inflammation in an evolutionary perspective: the contribution of cytokine genotype/phenotype to thriftiness. *Diabetologia* 42:1367–1374, 1999
4. Grimble RF: Inflammatory status and insulin resistance. *Curr Opin Clin Nutr Metab Care* 5:551–559, 2002
5. Pradhan AD, Ridker PM: Do atherosclerosis and type 2 diabetes share a common inflammatory basis? *Eur Heart J* 23:831–834, 2002
6. Saraheimo M, Teppo AM, Forsblom C, Fagerudd J, Groop PH: Diabetic nephropathy is associated with low-grade inflammation in type 1 diabetic patients. *Diabetologia* 46:1402–1407, 2003
7. Barzilay JI, Abraham L, Heckbert SR, Cushman M, Kuller LH, Resnick HE, Tracey RP: The relation of markers of inflammation to the development of glucose disorders in the elderly: the Cardiovascular Health Study. *Diabetes* 50:2384–2389, 2001
8. Stehouwer CD, Gall MA, Twisk JW, Knudsen E, Emeis JJ, Parving HH: Increased urinary albumin excretion, endothelial dysfunction, and chronic low-grade inflammation in type 2 diabetes; progressive, interrelated, and independently associated with risk of death. *Diabetes* 51:1157–1165, 2002
9. Festa A, D'Agostino R Jr, Howard G, Mykkanen L, Tracy RP, Haffner SM: Chronic subclinical inflammation as part of the insulin resistance syndrome: the Insulin Resistance Atherosclerosis Study (IRAS). *Circulation* 102:42–47, 2000
10. Fernández-Real JM, Ricart W: Insulin resistance and chronic cardiovascular inflammatory syndrome. *Endocrine Rev* 24:278–301, 2003
11. Pickup JC, Chusney GD, Thomas SM, Burt D: Plasma interleukin-6, tumor necrosis factor alpha and blood cytokine production in type 2 diabetes. *Life Sci* 67:291–300, 2000
12. Pradhan AD, Manson JE, Rifai N, Buring JE, Ridker PM: C-reactive protein, interleukin 6, and risk of developing type 2 diabetes mellitus. *JAMA* 286:327–334, 2001
13. Morohoshi M, Fujisawa K, Uchimura I, Numano F: Glucose-dependent interleukin-6 and tumor necrosis factor production by human peripheral blood monocytes in vitro. *Diabetes* 45:954–959, 1996
14. Esposito K, Nappo F, Marfella R, Giugliano G, Giugliano F, Ciotola M, Quagliaro L, Ceriello A, Giugliano D: Inflammatory cytokine concentrations are acutely increased by hyperglycemia in humans: role of oxidative stress. *Circ* 106:2067–2072, 2002
15. Yerneni KK, Bai W, Khan BV, Medford RM, Natarajan R: Hyperglycemia-induced activation of nuclear transcription factor κB in vascular smooth muscle cells. *Diabetes* 48:855–864, 1999
16. Hattori Y, Hattori S, Sato N, Kasai K: High-glucose-induced nuclear factor κB activation in vascular smooth muscle cells. *Cardiovasc Res* 46:188–197, 2000
17. Guijarro C, Egido J: Transcription factor-κB (NF-κB) and renal disease. *Kid Int* 59:415–424, 2001
18. Bierhaus A, Schiefofer S, Schwaninger M, Andrassy M, Humpert PM, Chen J, Hong M, Luther T, Henle T, Klöting I, Morcos M, Hofmann M, Tritschler H, Weigle B, Kasper M, Smith M, Perry G, Schmidt AM, Stern DM, Haring HU, Schleicher E, Nawroth PP: Diabetes-associated sustained activation of the transcription factor nuclear factor-κB. *Diabetes* 50:2792–2808, 2001
19. Morcos M, Sayed AA, Bierhaus A, Yfard B, Waldherr R, Merz W, Kloeting I, Schleicher E, Mentz S, Abd el Baki R, Tritschler H, Kasper M, Schwenger V, Hamann A, Dugi KA, Schmidt AM, Stern D, Ziegler R, Haering HU,

Andrassy M, van der Woude F, Nawroth PP: Activation of tubular epithelial cells in diabetic nephropathy. *Diabetes* 51:3532–3544, 2002
20. Lee FT, Cao Z, Long DM, Panagiotopoulos S, Jerums G, Cooper ME, Forbes JM: Interactions between angiotensin II and NF-kappaB-dependent pathways in modulating macrophage infiltration in experimental diabetic nephropathy. *J Am Soc Nephrol* 15:2139–2151, 2004
21. Bonizzi G, Karin M: The two NF-κB activation pathways and their role in innate and adaptive immunity. *Trends Immunol* 25:280–288, 2004
22. Hayden MS, Ghosh S: Signaling to NF-kappaB. *Genes Develop* 18:2195–2224, 2004
23. Pahl HL: Activators and target genes of Rel/NF-κB transcription factors. *Oncogene* 18:6853–6866, 1999
24. Senftleben U, Cao Y, Xiao G, Greten FR, Krahn G, Bonizzi G, Chen Y, Hu Y, Fong A, Sun SC, Karin M: Activation by IKKα of a second, evolutionary conserved NF-κB signaling pathway. *Science* 293:1495–1499, 2001
25. Xiao G, Harhaj EW, Sun SC: NF-κB-inducing kinase regulates the processing of NF-κB2/p100. *Mol Cell* 7:401–409, 2001
26. Israël A: The IKK complex: an integrator of all signals that activate NF-κB? *Trends Cell Biol* 10:129–133, 2000
27. Malinin NL, Boldin MP, Kovalenko AV, Wallach D: MAP3K-related kinase involved in NF-κB induction by TNF, CD95 and IL-1. *Nature* 385:540–544, 1997
28. Sharma K, McCue P, Dunn SR: Diabetic kidney disease in the db/db mouse. *Am J Physiol Renal Physiol* 284:F1138–F1144, 2003
29. Hanada T, Yoshimura A: Regulation of cytokine signaling and inflammation. *Cytokine Growth Factor Rev* 13:413–421, 2002
30. Wada T, Yokoyama H, Matsushima K, Kobayashi K: Monocyte chemoattractant protein-1: does it play a role in diabetic nephropathy? *Nephrol Dial Transplant* 18:457–459, 2003
31. Chow F, Ozols E, Nikolic-Paterson DJ, Atkins RC, Tesch GH: Macrophages in mouse type 2 diabetic nephropathy: correlation with diabetic state and progressive renal injury. *Kid Int* 65:116–128, 2004
32. Van Kooten C, Daha MR: Cytokine cross-talk between tubular epithelial cells and interstitial immunocompetent cells. *Curr Opin Nephrol Hypertens* 10:55–59, 2001
33. Daha MR, van Kooten C: Is the proximal tubular epithelial cell a proinflammatory cell? *Nephrol Dial Transplant* 15:41–43, 2000
34. Flyvbjerg A, Denner LA, Schrijvers BF, Tilton RG, Mogensen TH, Paludan SR, Rasch R: Long-term renal effects of a neutralizing RAGE-antibody in obese type 2 diabetic mice. *Diabetes* 53:166–172, 2004
35. Forbes JM, Cooper ME, Thallas V, Burns WC, Thomas MC, Brammar GC, Lee F, Grant SL, Burrell LA, Jerums G, Osicka TM: Reduction of the accumulation of advanced glycation end products by ACE inhibition in experimental diabetic nephropathy. *Diabetes* 51:3274–3282, 2002
36. Natoli G, Saccani S, Bosisio D, Marazzi I: Interactions of NF-κB with chromatin: the art of being at the right place at the right time. *Nat Immunol* 6:439–445, 2005
37. Marienfeld R, May MJ, Berberich I, Serfling E, Ghosh S, Neumann M: RelB forms transcriptionally inactive complexes with RelA/p65. *J Biol Chem* 278:19852–19860, 2003
38. Miyawaki S, Nakamura Y, Suzuka H, Koba M, Yasumizu R, Ikehara S, Shibata Y: A new mutation, aly, that induces a generalized lack of lymph nodes accompanied by immunodeficiency in mice. *Eur J Immunol* 24:429–434, 1994
39. Loverre A, Ditonno P, Crovace A, Gesualdo L, Ranieri E, Pontrelli P, Stallone G, Infante B, Schena A, Di Paolo S, Capobianco C, Ursi M, Palazzo S, Battaglia M, Selvaggi FP, Schena FP, Grandaliano G: Ischemia-reperfusion induces glomerular and tubular activation of proinflammatory and antiapoptotic pathways: differential modulation by rapamycin. *J Am Soc Nephrol* 15:2675–2686, 2004
40. Lernbecher T, Kistler B, Wirth T: Two distinct mechanisms contribute to the constitutive activation of RelB in lymphoid cells. *EMBO J* 13:4060–4069, 1994
41. Bren GD, Solan NJ, Miyoshi H, Pennington KN, Pobst LJ, Paya CV: Transcription of the RelB gene is regulated by NF-κB. *Oncogene* 20:7722–7733, 2001
42. Xia Y, Pauza ME, Feng L, Lo D: RelB regulation of chemokine expression modulates local inflammation. *Am J Pathol* 151:375–387, 1997
43. Weih F, Carrasco D, Durham SK, Barton DS, Rizzo CA, Ryseck RP, Lira SA, Bravo R: Multiorgan inflammation and hematopoietic abnormalities in mice with a targeted disruptiion of RelB, a member of the NF-κB/Rel family. *Cell* 80:331–340, 1995
44. Xia Y, Chen S, Wang Y, Mackman N, Ku G, Lo D, Feng L: RelB modulation of IκBα stability as a mechanism of transcription suppression of interleukin-1α (IL-1α), IL-1β, and tumor necrosis factor alpha in fibroblasts. *Mol Cell Biol* 19:7688–7696, 1999
45. Jacque E, Tchenio T, Piton G, Romeo PH, Baud V: RelA repression of RelB activity induces selective gene activation downstream of TNF receptors. *Proc Natl Acad Sci* 102:14635–14640, 2005
46. Lawrence T, Beblen M, Liu GY, Nizer V, Karin M: IKKα limits macrophage NF-κB activation and contributes to the resolution of inflammation. *Nature* 434:1138–1143, 2005